Journal of Solid State Electrochemistry
https://doi.org/10.1007/s10008-023-05742-0

ORIGINAL PAPER

Influence of LiCl on the kinetics of Mg^{2+} insertion into TiO_2 prepared by solid-state chemical reaction

Gulmira Rakhymbay[1] · Khaisa Avchukir[1] · Yedil Konysbay[1] · Florence Vacandio[2] · Raigul Jumanova[1] · Yeldana Bakhytzhan[1] · Ainaz Abildina[1] · Akmaral Argimbayeva[1]

Received: 15 August 2023 / Revised: 4 October 2023 / Accepted: 4 November 2023
© The Author(s), under exclusive licence to Springer-Verlag GmbH Germany, part of Springer Nature 2023

Abstract

In this study, TiO_2 was prepared via a solid-state chemical reaction and used as an anode for magnesium/lithium hybrid-ion batteries. The X-ray diffraction characterization of the synthesized titanium dioxide demonstrated that the material consists of 10% TiO_2(B) and 90% anatase phases. Cyclic voltammetry and electrochemical impedance spectroscopy (EIS) measurements showed the lowest charge transfer resistance and the highest capacity for batteries assembled with 9 mM LiCl because of the activation effect of the Cl^- anion. In general, TiO_2 as anode material in Mg^{2+}/Li^+-ion mixed solutions demonstrated sluggish electrochemical kinetics and a rate constant obtained from the EIS data of 1.05×10^{-8} cm s^{-1}. From the cyclic voltammetry measurements, it was found that the capacity of the magnesium-lithium battery has more pseudocapacitance characteristics than the mixed-controlled process, as in other studies. The investigated TiO_2||0.05 M $Mg(ClO_4)_2$ + 0.009 M LiCl/AN||Mg hybrid-ion battery demonstrated a capacity of approximately 25 mAh g^{-1} after 50 cycles at 35 mA g^{-1} current.

Keywords Magnesium ion batteries · Titanium dioxide · Solid-state chemical reaction · Diffusion coefficient · Electrochemical impedance spectroscopy

Introduction

Multivalent-ion batteries are a promising type of electrochemical-energy storage device with applications in various fields such as transportation, renewable energy, and portable electronics [1–4]. Magnesium ion batteries (MIB) are attractive polyvalent batteries owing to their high volumetric capacity, low cost, and safety [5–7]. However, MIBs still have several scientific problems associated with the lack of high-performance electrode materials and are unsuitable for aqueous electrolytes. In addition, the slow diffusion of Mg^{2+} ions in solids hinders their practical applications [2, 8–10]. The literature presents works [11–13] that try to solve this problem with the help of a hybrid-ion battery. Su and Gao [14, 15] proposed a Li^+/Mg^{2+} hybrid-ion battery (LMIB) consisting of a lithium cathode, magnesium anode, and Li^+/Mg^{2+} non-aqueous hybrid electrolyte. During battery cycling, Li^+ intercalation/deintercalation processes occur at the cathode, and Mg precipitation/dissolution occurs at the anode. It has been found that the Li^+/Mg^{2+} hybrid battery exhibits the best overall performance (specific capacity, specific energy, cyclic stability, and performance) among all the known MIBs because of the combination of the advantages of these materials. Azmi et al. present [12] the reversible behavior of batteries based on crystallized TiO_2-type electrodes, namely, TiO_2-anatase and TiO_2(B), in "all phenyl" complexes (APC)/LiCl hybrid electrolytes and found that, in comparison with pure APC electrolyte, crystallized TiO_2 electrodes provide a high charge/discharge capacity in the hybrid electrolyte. In situ synchrotron diffraction clearly shows that in the APC/LiCl hybrid electrolyte, anatase TiO_2 undergoes structural changes through a solid solution and two-step reaction mechanism, while TiO_2(B) exhibits only one solid solution reaction during charge/discharge processes. In addition, the results of the X-ray photoelectron spectroscopy (XPS) analysis of anatase TiO_2 and TiO_2(B) cathodes confirm the changes in the Mg/Ti and Li/Ti ratios at different stages, indicating the contribution of Mg and Li to the charge accumulation mechanism in the hybrid electrolyte.

✉ Khaisa Avchukir
khaisa.avchukir@cfhma.kz

[1] Center of Physical Chemical Methods of Research and Analysis, Al-Farabi Kazakh National University, Tole bi 96A, Almaty 050012, Kazakhstan

[2] Aix-Marseille University, CNRS, MADIREL, UMR 7246, Marseille cedex 20, 13397, France

Published online: 18 November 2023

Titanium dioxide is a non-toxic, environmentally friendly, and cost-effective material compared to some other electrode materials [16–19], which can be important for large-scale battery production. However, TiO_2 may perform poorly at high charge/discharge rates due to its low conductivity, which makes it less suitable for applications requiring fast energy transfer. Meng et al. [11] showed in their studies that TiO_2(B) is not suitable for Mg^{2+} intercalation due to the difficulty of Mg^{2+} desolvation and large diffusion barrier. According to the electrochemical impedance spectroscopy results, the charge transfer resistance of TiO_2(B) in an electrolyte containing Mg^{2+} ions is much higher than that in the Li^+/Mg^{2+} hybrid electrolyte. This indicated that the dominant reaction in the TiO_2(B) electrode was the intercalation of Li^+ ions, accounting for approximately 74% of the total capacitance. This paper reveals the different mechanisms of energy accumulation of magnesium and lithium ions in the TiO_2(B) structure, and also shows the prospect of using traditional materials for storing Li^+ in the creation of LMIB.

The intercalation properties of materials with respect to magnesium ions can be enhanced by modifying the electrolyte or pre-treating the material with specific compounds. For instance, treating the active material with a chloride ion-rich solution is a simple and cost-effective method that has been found to improve the intercalation properties. Cl-based compounds in the electrolyte also play a crucial role in electrochemical intercalation processes [20]. Attias et al. demonstrated the role of Cl^- ions in the intercalation of Mg ions in the Chevrel phase (CP). The addition of chlorine-containing compounds to the electrolyte facilitated the intercalation of magnesium. In addition, the proposed mechanism of Mg intercalation in CP emphasizes the importance of chlorine-based compounds in charge transfer across the solid/solution interface.

The replacement of metallic Mg with other negative electrodes that must be compatible with conventional electrolytes may also pave the way for the efficient emergence of Mg-ion batteries as reliable alternatives to lithium-based systems. Previous studies [1, 21–24] have found that elements such as Sn, Sb, Pb, and Bi at low potentials form intermetallic compounds with Mg, leading to high volume capacities. However, only bismuth-based systems exhibit highly reversible behaviors and long lifetimes. The Sn- and Sb-based systems suffer from rapid capacity degradation, and the Pb-coated electrodes show extremely low Coulombic efficiencies, indicating electrolyte decomposition reactions on the Pb surface during cycling. Recently, Murgia and Weldekidan investigated indium-based electrodes in Mg batteries and demonstrated the electrochemical activity of In micrometer powder in a Mg battery with an electrolyte based on an organohaloaluminate compound [9]. Both the In and MgIn electrodes show good cycling performances; however, at higher rates, they present a quick capacitance decrease.

In recent years, nanostructured materials with various morphologies (nanoparticles, nanotubes, and nanowires) have been intensively studied as electrode materials for electrochemical energy-storage devices [25]. Many researchers have found that one of the promising candidates for anodes in lithium-ion batteries is titanium dioxide, owing to several advantages, such as low cost, safety, and low toxicity [26–28]. Despite the limited practical capacity of Li^+ ions for nano-anatase, it has been found in previous studies [24] that TiO_2(B) nanowires have capacitances greater than 250 mAh g^{-1}. The electrochemical incorporation of Li into nano-sized rutile TiO_2 synthesized using a glycerol-modified Ti precursor and an anionic surfactant as a structurant was studied [26]. It exhibits high charge/discharge capability and remarkable stability, making it a promising anode material for high-power lithium-ion batteries.

The principle of MIB and LIB operations is based on the reversible intercalation/deintercalation of magnesium ions at the cathode and anode. Wu et al. [29] reported that as an anode in MIB, $Li_4Ti_5O_{12}$ nanoparticles (LTO NPs) exhibit excellent cycling performances (capacity retention of more than 95% over 500 cycles) due to the negligible volume change occurring during the intercalation/deintercalation of magnesium ions process after the initial activation. In addition, it was found that the size of the LTO particles influences the electrochemical behavior of MIB during magnesium storage. Highly reversible introduction and extraction of Mg ions into the electrode were ensured only when the LTO particle size was below 40 nm. In [30], a three-dimensional microporous $Na_2Ti_6O_{13}$ (NT6) electrode exhibited better electrochemical characteristics than layered $Na_2Ti_3O_7$ (NT3) nanowires. This is because NT6 has a three-dimensional microporous structure and regular structural unit of TiO_6 octahedra, which leads to stability during the magnesiation and demagnesiation processes. In summary, Ti-based composites are the main objects of study for the possible use of metal oxides as anodes for MIBs. They deliver excellent cycling performance owing to their low-strain characteristics. However, their specific capacities are generally low.

In previous works, we investigated the intercalation of magnesium on TiO_2 synthesized by the hydrothermal method and on titanium oxide nanotubes obtained by the anodic oxidation of titanium [31, 32]. In both cases, the possibility of Mg intercalation through these materials in $Mg(TFSI)_2$ in ethylene carbonate (EC)/dimethyl carbonate (DMC) electrolytes was established. In the case of the tubular structure TiO_2, the material capacity was very low and could only be used as a microbattery. In this study, the possibility of improving the capacitance characteristics of titanium oxide by modifying its electrolyte was investigated. The authors of [33] found that LiCl could dissolve insoluble $MgCl_2$ deposits and activate the solid/electrolyte interface when added to the

$[Mg{\cdot}6THF][AlCl_4]_2$ electrolyte, thereby reducing the electrochemical overpotential of the Mg electrode and exhibiting a long cycling performance in Mg/S cell.

In this study, we investigated the electrochemical performance of TiO_2(B)/anatase-based composite anodes in $MgClO_4$/LiCl hybrid electrolytes. The anode material (TiO_2(B)/anatase) was synthesized using a novel solid-state chemical reaction method. Compared to the traditional hydrothermal method, in the solid-state chemical reaction method, the precursor is synthesized at room temperature and then calcined in air at atmospheric pressure, which allows a significant increase in the synthesis time [34, 35].

Experimental

Synthesis of titanium dioxide by solid-state chemical reaction

TiO_2(B)/anatase was synthesized by a solid-state chemical method. Titanium oxysulfate sulfuric acid hydrate ($TiOSO_4{\cdot}xH_2SO_4{\cdot}xH_2O$) and oxalic acid ($H_2C_2O_4{\cdot}2H_2O$) were supplied by Sigma-Aldrich and used as received. For the synthesis of TiO_2(B)/anatase, 0.1 mol of $TiOSO_4{\cdot}xH_2SO_4{\cdot}xH_2O$ was weighed. Then, 0.15 mol of $H_2C_2O_4{\cdot}2H_2O$ was added to $TiOSO_4{\cdot}xH_2SO_4{\cdot}xH_2O$ and ground in a ball mill for 1 h at 25 °C, at 100 revolutions, 10-min work, 5-min rest, and 6 cycles. The powder was heated in a water bath overnight (12 h) at 70 °C to ensure a complete reaction; this was the precursor. Subsequently, the precursor was calcined at 550 °C for 3 h at a heating rate of 5 °C per minute. The calcined product was washed with deionized water in a buncher funnel until the pH was neutral and dried in a vacuum dryer at 40 °C for 12 h.

The synthesis process consists in the following [36]:

$$TiOSO_4 \cdot xH_2SO_4 \cdot xH_2O + H_2C_2O_4 \cdot 2H_2O = TiOC_2O_4 + H_2SO_4 + H_2O$$

$$TiOC_2O_4 = TiO_2 + CO_2 + CO$$

Preparation of the electrode

Electrodes were formulated by mixing the TiO_2(B)/anatase composite oxides with 10 wt.% of carbon black (Y50A; Saft) and 10 wt.% of polyvinylidene fluoride (PVDF; Solvay, Solef 5130). *N*-Methyl-2-pyrrolidone (NMP, 99%; Sigma-Aldrich) was used as the solvent.

The obtained slurry was stirred for an hour at 1000 rpm and then casted onto a nickel substrate. To ensure good adhesion between the substrate and the anode layer, contaminants were removed from the surface of the substrate using abrasive paper and degreased with ethyl alcohol. In this process, the prepared anode quantity was poured onto a nickel substrate in front of the Doctor Blade and the blade was manually moved forward, stretching the ink and forming a film of a given thickness (50–100 µm). After applying the coating to evaporate the solvent residues from the surface, the electrode was pre-dried in a vacuum oven (BOYN) for 6 h at a temperature of 40 °C and then for 12–48 h gradually increasing the temperature to 100 °C. Finally, TiO_2 electrodes with a diameter of 0.94 cm were obtained, and the mass of active material on the current collector per unit area was 16.57 mg/cm^2. Disk electrodes with a geometrical surface area of 0.694 cm^2 were cut and stored in a glove box (Ossila).

Characterization

The morphologies of synthesized TiO_2(B)/anatase were characterized by SEM, and Fig. 1 shows the results. It is apparent that the products consisted of uniform, long, and slim tubes and a large ratio of length to diameter (red cycle). The TiO_2 nanotubes are clear and dispersed. A large amount of these particles are microspheres and are obviously agglomerated (green cycle). The size and shape of the particles are uniform. The composite oxides are agglomerated to cauliflower-like aggregates of several micrometers, thus favoring the contact between the active material and the electrolyte. In summary, the applied synthesis protocol offers a reproducible and versatile access to nanoscale particles with a good control of the resulting physical properties (structure and morphology) of the material.

The X-ray diffraction (XRD) pattern of a TiO_2 synthesized by solid-state chemical reaction is shown in Fig. 2a. According to literature [37], the peaks at 36.1° correspond to the main peak of TiO_2(B) (JCPDS No. 74-1940). The XRD pattern of the TiO_2 sample shows noticeable diffraction peaks at values of 2θ values of approximately 25.3°, 37.9°, and 48.1°, which correspond to the (101), (004), and (200) anatase phases, respectively. In addition, weaker peaks were observed at values of 2θ approximately 36.1° and 56.6°, corresponding to the (110) and (210) planes of the TiO_2(B) phase, respectively. The intensities of the peaks suggest that the sample consisted of approximately 90% anatase and 10% TiO_2(B) phases. The peaks are relatively sharp, which indicates good crystallinity. Quantitative phase analysis confirmed the phase composition as shown in Fig. 2b. The results of the XRD analysis shown in Fig. 2 indicate that TiO_2(B) was successfully synthesized via the solid-state chemical reaction.

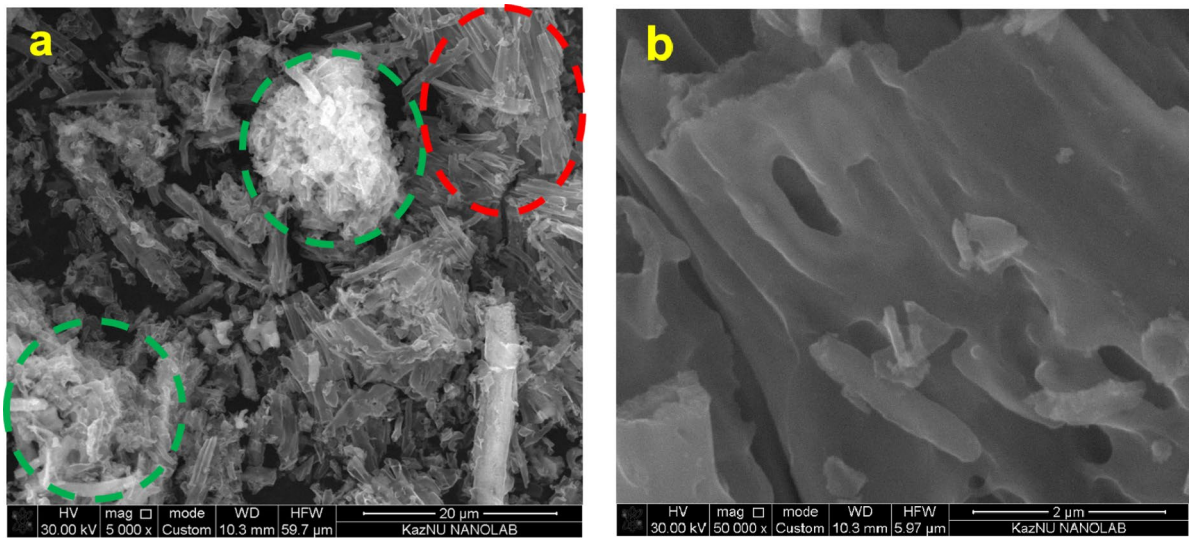


Fig. 1 SEM image of the synthesized TiO_2(B)/anatase material, at different magnifications: 5000× (**a**); 50,000× (**b**)

Electrochemical experiments

Electrochemical behavior of the TiO_2 prepared by solid-phase chemical reaction was examined in "coating cell" type three-electrode electrochemical cell. Mg rods with a diameter of 5 mm were used as the counter and pseudo-reference electrodes. The working electrode was prepared from a paste containing TiO_2 (80 wt.%) and carbon black (Y50A; Saft) (10 wt.%) conductive additive *N*-methyl-2-pyrrolidone (NMP, 99%; Sigma-Aldrich) as solvent, and polyvinylidene fluoride (PVDF; Solvay, Solef 5130) (10 wt.%) as binder. This paste was deposited on a nickel current collector (see the procedure of the preparation given in "Preparation of the electrode" section). Magnesium perchlorate solution with different concentrations—0.05 M, 0.10 M, and 0.15 M/acetonitrile—was used as the Mg^{2+} ion electrolyte (MIB). A Mg^{2+}/Li^{+} hybrid electrolyte (MLIB) was prepared by adding various amounts of LiCl. For comparison, the electrochemical behavior of the TiO_2 in MLIB was studied by varying the LiCl concentration from 6.25 to 25 mM. Cyclic voltammetry (CV), charge–discharge measurements, and electrochemical impedance spectroscopy (EIS) experiments were performed using an Autolab 302N potentiostat–galvanostat and a Bio-Logic SP300 electrochemical workstation. The impedance measurements were obtained in a frequency range from 100 kHz to 10 mHz using an AC voltage with a 10-mV amplitude versus open-circuit voltage (OCV).

Results and discussion

Discharge and ionization of magnesium from $Mg(ClO_4)_2$ electrolyte

The electrochemical behavior of TiO_2 was studied in $Mg(ClO_4)_2$ solvated in acetonitrile (AN) electrolyte at different Mg^{2+} concentrations. Figure 3a shows the voltammograms obtained for the discharge-ionization of magnesium in a 0.05 M $Mg(ClO_4)_2$ electrolyte. As shown in Fig. 3a, the CV curves of Mg discharge-ionization show no peaks. Therefore, the absence of a faradaic current demonstrates the impossibility of electrochemical reduction (or insertion) and dissolution of magnesium ions from an acetonitrile environment containing $Mg(ClO_4)_2$ salt on the surface of the composite electrode containing 80% TiO_2.

The CV curves of TiO_2 at different scan rates (Fig. 3a) show a direct correlation between the area of the CV curve and the scan rate, which is typical for non-Faradaic processes (charge–discharge of the double layer). However, in a previous study [38, 39], the CV of the V_2O_5 electrode in 0.1 M $Mg(ClO_4)_2$/AN electrolyte clearly presented both anodic and cathodic peaks. The electrolyte containing the weaker anion ($Mg(TFSI)_2$) has an anodic peak with a lower height, which is in agreement with the nature of the anion. Furthermore, an electrolyte based on acetonitrile demonstrated much higher current densities than ethylene carbonate/dimethyl carbonate (EC/

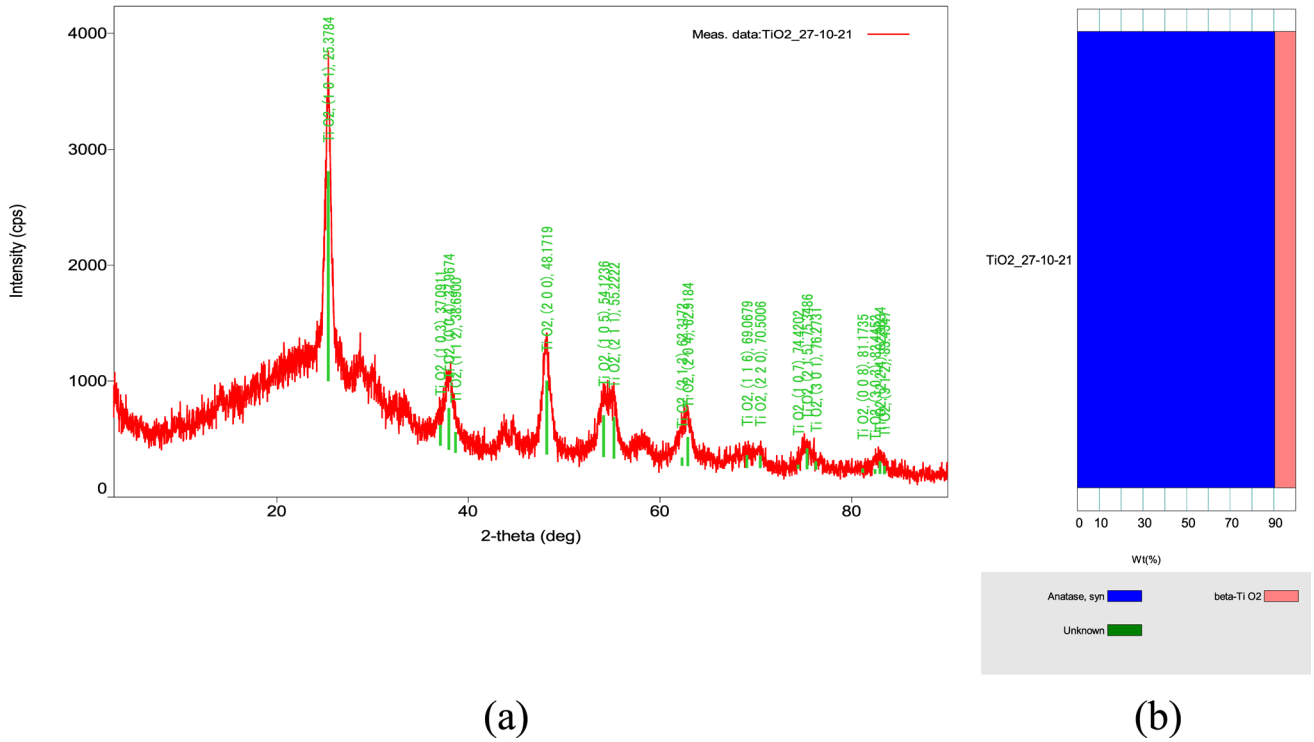


Fig. 2 XRD spectra of the powder obtained by solid-state synthesis—**a** distribution of the anatase and **b** forms of the synthesized TiO_2

DMC) mixed solvent. The addition of chlorides to the electrolyte promotes reversible Mg intercalation with comparatively fast kinetics [20]. In addition, in the aforementioned work, the authors suggested a comprehensive Mg ion intercalation mechanism scheme for Chevrel-phase-based electrode materials. However, there is a paucity of studies on the activation effect of chloride anions on the discharge and ionization of magnesium ions in TiO_2-based material. Figure 3b shows the influence of Cl^- anions on the electrochemical behavior of Mg in the AN electrolyte. The pure solvent AN (curve i) and an electrolyte containing 0.009 M LiCl (curve ii) exhibited pure non-faradaic behavior; in contrast, in the presence of magnesium perchlorate, a cathodic peak appeared (curve

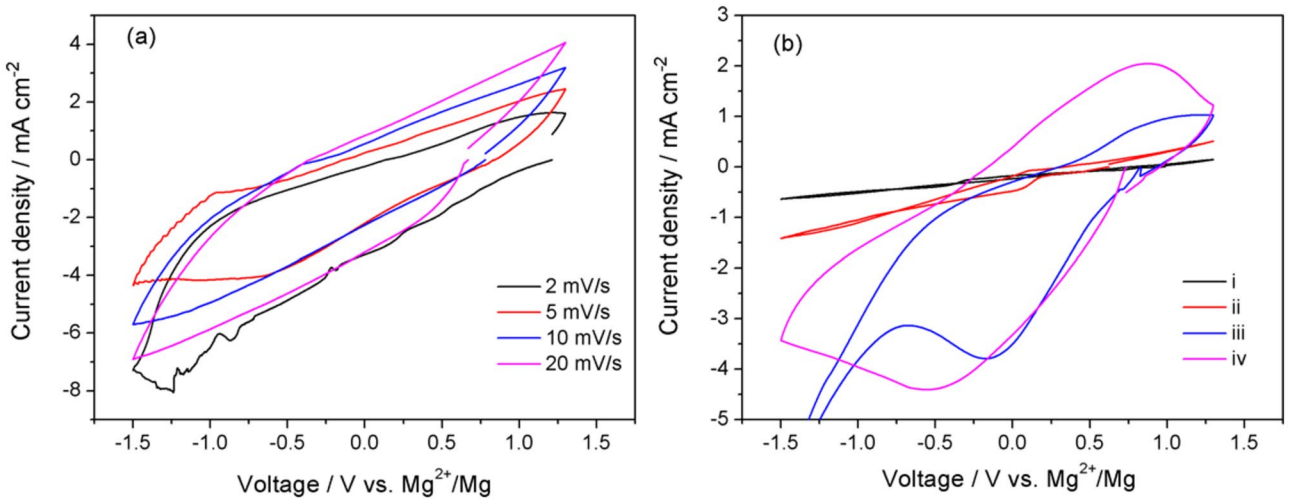


Fig. 3 Cyclic voltammetry (CV) curves of TiO_2 in 0.05 M $Mg(ClO_4)_2$/AN electrolyte at different scan rates (**a**); CV curves of TiO_2 in pure AN (*i*), 0.009 M LiCl in AN (*ii*), 0.05 M $Mg(ClO_4)_2$ in AN (*iii*), and 0.05 M $Mg(ClO_4)_2$+0.009 M LiCl electrolyte (*iv*) (**b**). The geometric area of the electrode surface was 0.694 cm^2, and the mass of the composite material (80% TiO_2) per unit area was approximately 0.0166 g/cm^2

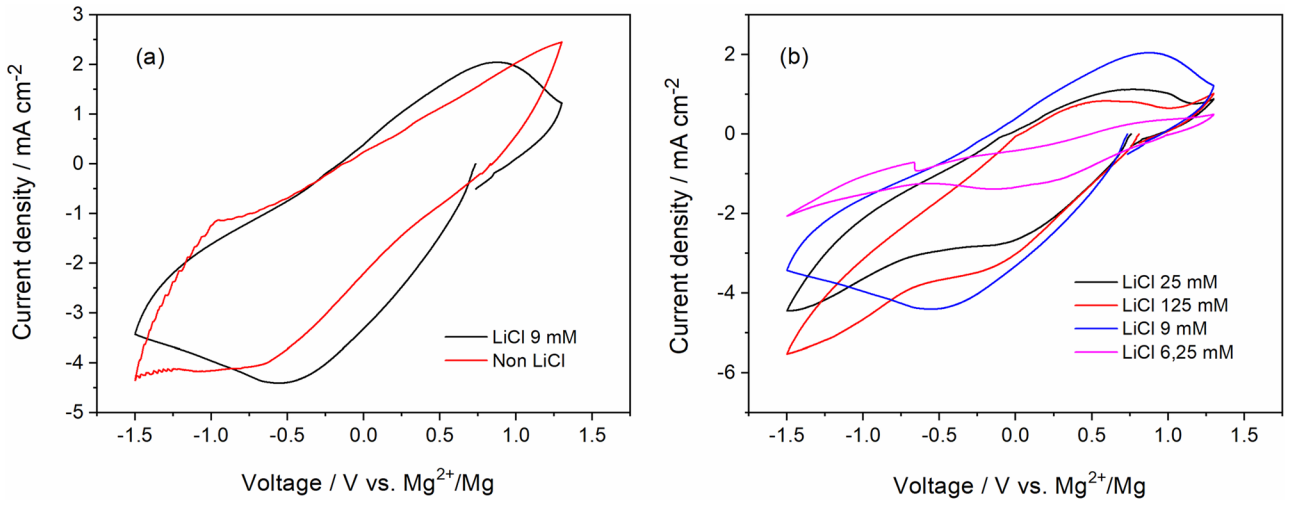


Fig. 4 Cyclic voltammograms of TiO_2/Ni electrode at 2 mV/s scan rate. **a** Electrolyte containing 0.05 M $Mg(ClO_4)_2$ in the absence and in the presence of 0.009 M LiCl (black solid line) in AN. **b** Mixed electrolyte containing 0.05 M $Mg(ClO_4)_2$ and different concentrations of LiCl from 6.25 to 25 mM in AN

iii). Furthermore, it is obvious from the cyclic voltammogram of 0.05 M $Mg(ClO_4)_2$ solution that curve iii has a weak anodic peak, which demonstrates weak reversibility against Mg. In addition, in the presence of a small amount of chloride anions (curve iv), the areas of both anodic and cathodic peaks increased significantly. This "activation" effect of chloride anions can be explained by the formation of a strongly absorbed complex layer, as suggested in [20].

The cyclic voltammograms of the perchlorate electrolyte do not close after the first cycle; this is especially visible at low scanning rates (Fig. 3a). Thus, at low scan rates, the surface of the electrode material changes noticeably during long-term measurements. In our case, it is clear from the CV curve that the capacity decreased slightly. This may be due to the formation of a solid electrolyte interphase (SEI) film on the electrode surface, the poor deintercalation of magnesium ions, and other parasitic processes occurring at the electrode/electrolyte interface. However, it can be seen from the CV curve in Fig. 4a that this effect disappears in the presence of chloride ions. Adding chloride ions to a perchlorate solution, on the contrary, slightly increases the capacity of the material, apparently partially dissolving the film formed by SEI and improving the intercalation of electrochemically active particles (magnesium and lithium ions).

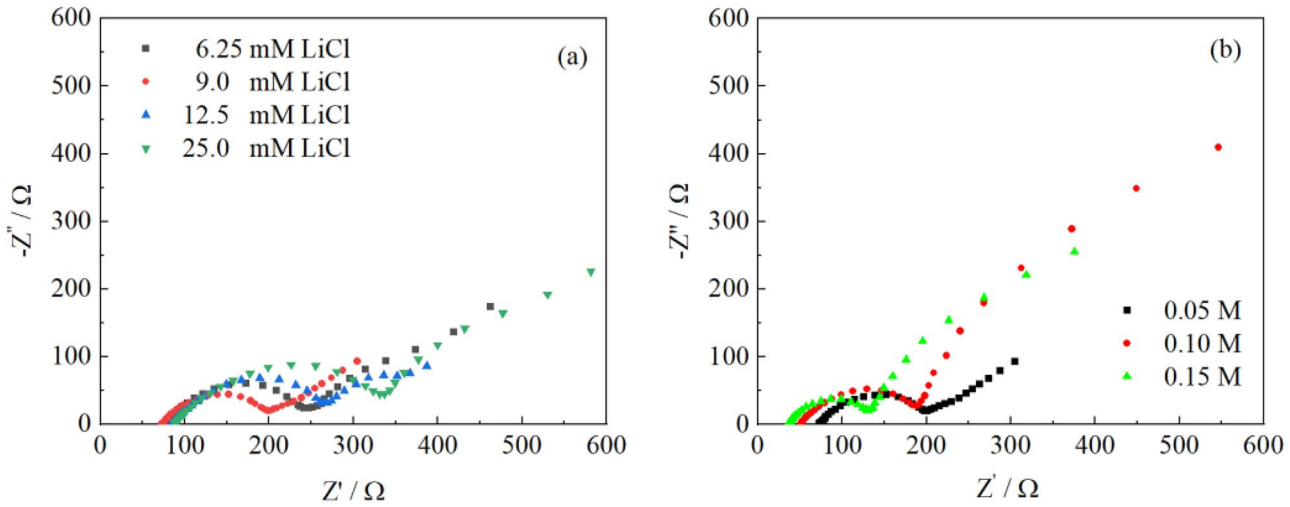


Fig. 5 **a** Nyquist plots of the TiO_2 in 0.05 M $Mg(ClO_4)_2$ in AN electrolyte at different concentrations of LiCl. **b** Nyquist plots of the TiO_2 in 9 mM LiCl + AN at different concentrations of $Mg(ClO_4)_2$

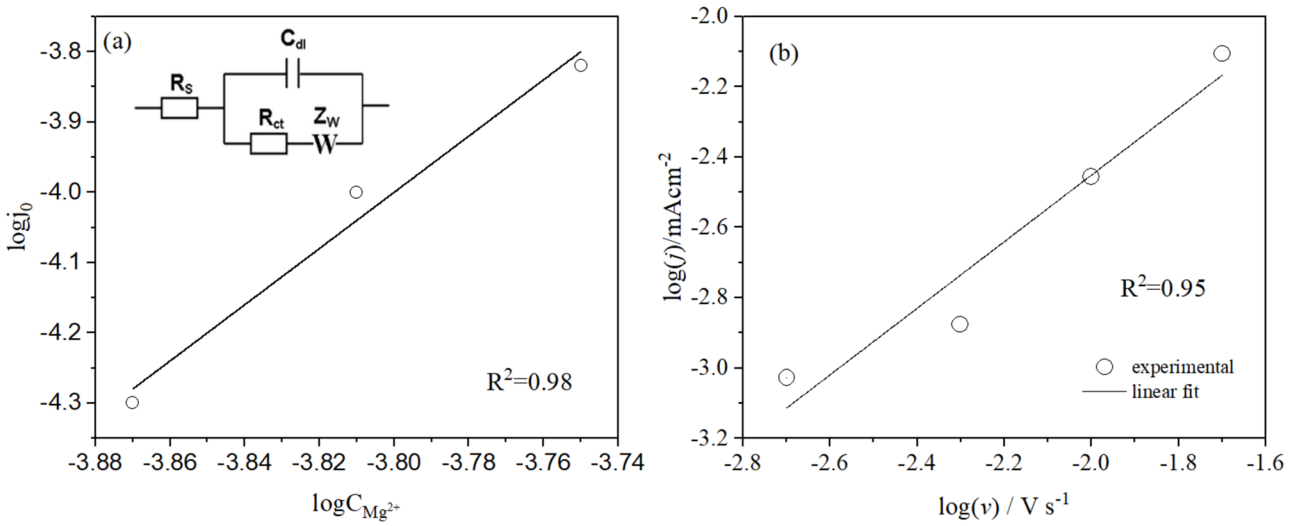


Fig. 6 **a** The dependence $\log j_0 - \log C_{Mg^{2+}}$. Insert: electrical equivalent circuit of the Randles. **b** log(*j*) vs. log(*v*), where *j* is a cathodic current density at 0 V potential vs. Mg/Mg^{2+}, at different scan rates, respectively

The influence of the lithium chloride concentration on the charge transfer stage of the discharge/ionization reaction of Mg ions across the solution/host interface is discussed in the following section.

Electrochemical properties of the TiO_2/Ni material in magnesium/lithium mixed electrolyte

The electrochemistry of the TiO_2/Ni electrode was initially studied using cyclic voltammetry under different conditions. The pure perchlorate electrolyte gave a weak cathodic peak at −0.7 V versus pseudo-Mg reference electrode; at the same time, there is no clear anodic peak up to +1.25 V potential. Addition of small amount of lithium chloride shifts cathodic peak from −0.7 to −0.5 V and there is an anodic peak at +0.75 V (Fig. 4a). The presence of a 9-mM chloride anion decreased the difference between the anodic and cathodic peak currents by increasing the reversibility of magnesium insertion into TiO_2. However, considering that the difference in the peak potentials (ΔE_p) is approximately 1.20 V, the insertion-disinsertion of magnesium ions into titanium dioxide is not a reversible process. The influence of LiCl concentration on the reversibility of magnesium discharge-ionization is shown in Fig. 4b.

The CVs of TiO_2 demonstrate the absence of a direct correlation between the chloride anion concentration and cathodic peak current density (j_{pc}). A direct correlation was observed only at a low concentration range of up to 9 mM. Further increases in the Cl^- concentration led to a decrease in j_{pc}. Moreover, the dependence between the j_{pc} and C_{LiCl} was characterized by a maximum chloride ion concentration of approximately 9 mM. The CV results were in good agreement with those obtained by electrochemical impedance spectroscopy. The electrochemical impedance curves of the TiO_2 electrodes with different lithium chloride concentrations are shown in Fig. 5.

The Nyquist plots for TiO_2 present a semicircle with a diameter equal to the charge transfer resistance and a linear part owing to diffusion limitation. The impedance of TiO_2 at low frequencies is linear, which allows calculation of the diffusion coefficient of magnesium ions from the value of the Warburg impedance [40]. The values of the electrolyte resistance, charge-transfer resistance, double-layer capacitance, and diffusion coefficients were obtained by fitting the experimental curves using a simple Randles equivalent circuit (Fig. 6a insert). The obtained values are listed in Table 1.

The EIS results show that the electrolyte with a 9-mM LiCl concentration has the lowest resistance to charge transfer (97.1 Ω cm^2) and the highest capacitance. Hence, this composition was selected for further study. To determine the rate constant of the electrochemical reaction, EIS was performed for TiO_2 in AN at various magnesium perchlorate

Table 1 The values of electrolyte resistance (R_s), charge-transfer resistance (R_{ct}), double-layer capacitance (C_{dl}), and diffusion coefficients of magnesium ions ($D_{Mg^{2+}}$) at the electrochemical discharge-ionization of the magnesium from 0.05 M $Mg(ClO_4)_2$ in AN electrolyte

C_{LiCl}, mM	R_s, Ω cm^2	R_{ct}, Ω cm^2	C_{dl}, μF cm^{-2}	$D_{Mg^{2+}}$, × 10^{-11} cm^2 s^{-1}
6.25	53.9	133.2	1.99	28.05
9.00	50.4	97.1	11.73	29.00
12.50	59.6	145.2	2.68	23.10
25.00	62.7	203.3	0.56	6.05

Table 2 The values of the exchange current density (j_0), R_{ct}, and $D_{Mg^{2+}}$

$C_{Mg(ClO_4)_2}$, M	R_{ct}, Ω cm^2	j_0, 10^{-4} Acm^{-2}	$D_{Mg^{2+}}$, $\times 10^{-11}$ cm^2 s^{-1}
0.05	97.1	1.32	29.00
0.10	82.5	1.56	0.51
0.15	71.7	1.79	0.45

concentrations (Fig. 5b). All the parameters are presented in Table 2.

The values of for exchange current density, j_0, were obtained using the following equation:

$$j_0 = \frac{RT}{nFR_{ct}}$$

where R is the gas constant, T is the absolute temperature (K), n is the number of electrons involved in the electrode process, F is the Faraday constant, and R_{ct} is the charge-transfer resistance (Ω cm^2).

The values of j_0 reported in Table 2 were calculated using $n=2$, but this does not mean a charge transfer of two electrons in one elemental electrochemical act. Therefore, the electrochemical reduction of Mg should be perceived as a complex multistage electrochemical process. Moreover, there is a possible method for Mg insertion by the reduction/oxidation process via one electron of the TiO_2 species ($Ti^{4+} \rightleftarrows Ti^{3+}$), analogous to the insertion of Li^+ cations in lithium-ion batteries. It should be clarified that in all calculations, the electrochemical reaction is considered as follows:

$$Mg^{2+} + 2e^- \leftrightarrows Mg^0$$

The dependence between the exchange current density and the rate constant (k_s^{exp}) of the above reaction can be expressed by the following equation:

$$j_0 = nFk_s^{exp}\left(C_{Mg^{2+}}\right)^{1-\alpha}\left(C_{Mg}\right)^{\alpha}$$

If we neglect the activity of the reduced form (C_{Mg}) and take the logarithm, the following expression for the exchange current density makes it possible to determine the reaction rate constant:

$$\log j_0 = \log\left(nF\,k_s^{exp}\right) + (1-\alpha)\log C_{Mg^{2+}}$$

The measured rate constant of charge transfer was calculated from the linear dependence $\log j_0 - \log C_{Mg^{2+}}$ (Fig. 6a) using the above equation as shown in [40].

The value of k_s^{exp} determined by the EIS method is 1.05×10^{-8} cm s^{-1}, which is two orders of magnitude lower than that of the TiO_2 electrode prepared by the hydrothermal method (1.29×10^{-6} cm s^{-1}) [32]. Here, it may seem that titanium oxide obtained by the hydrothermal method in $Mg(TFSI)_2$/AN medium has more reversible kinetics and relatively fast diffusion of magnesium ions, 1.56×10^{-8} cm^2 s^{-1}, than in this study (Table 2). However, attention should be paid to the method for determining the kinetic parameters of the reaction, since in [32] cyclic voltammetry was used, which does not allow compensation for the concentration overvoltage caused by slow mass transfer, as described in [40], in which case, the results obtained by the EIS method can be considered the most accurate. The rotating disk electrode technique can be used for the most accurate determination of the diffusion coefficient, as shown in [41]. However, in our case, the application of this method seems to be difficult because of the non-planarity of the electrode surface and the complexity of the material composition. In addition, the influence of the concentration of magnesium ions on the current–voltage characteristics was studied using CV (Fig. 7a).

The cyclic voltammograms of the MRB cell indicate a favorable effect of an increase in the concentration of the magnesium electrolyte on the charge–discharge currents. The absence of clear cathodic and anodic peaks makes it difficult to use CV to determine kinetic data. In addition, when the scan rate increased, the peaks became unclear and completely disappeared at 20 mV/s at high magnesium ion concentrations (0.1 and 0.15 M). However, at low concentration, the cathodic peaks was more distinguishable (Fig. 7b). Similar CV characteristics can be given by electrodes with a large active surface, i.e., systems with large capacitive currents. One example of such a system is activated carbon materials with a sufficiently large active surface (approximately 2800 m^2 g^{-1} [42]), which, when used for gold electrosorption, showed similar voltammograms (Fig. 4b [43]). To clarify the nature of the current and determine the contribution of the capacitance to the total current, the CV of the MRB cell was analyzed at various scan rates (Fig. 7b). For this purpose, the dependence log(j)–log(v) was obtained from the slope–b of the linear dependence, which was given in a similar manner as indicated in the literature [31], according to the power-law relationship of the peak current with the scan rate [44]:

$$j = av^b$$

where a is a constant and v is the potential sweep rate.

The logarithm of this dependence made it possible to calculate the values of b from the slope of the linear dependence of log(j) versus log(v) (Fig. 6b). In Fig. 7b, the reduction peaks of the $Mg(ClO_4)_2$/LiCl solution shifted with increasing potential sweep rate because of the diffusion-controlled nature of the electrode process. The b-value can change from 0.5 to 1 depending on the nature of the measured current. Diffusion-controlled electrochemical reactions have a b-value of 0.5, and if the value of the b coefficient is close

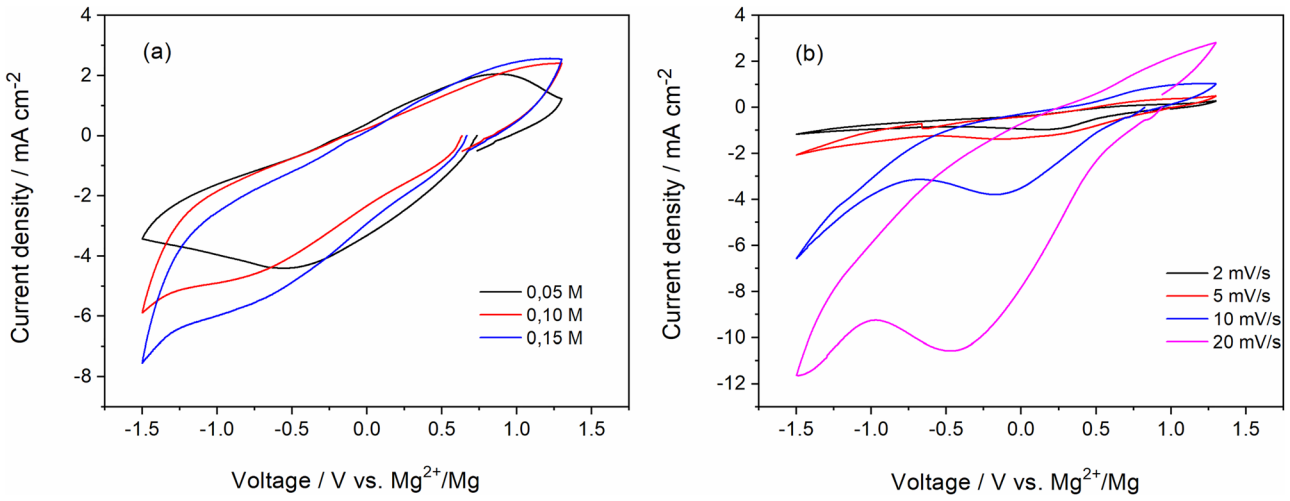


Fig. 7 Cyclic voltammograms of TiO_2/Ni electrode **a** at different concentrations of $Mg(ClO_4)_2$ in the presence of 0.009 M LiCl at 2 mV/s scan rate; **b** at different scan rates, electrolyte: 0.05 M $Mg(ClO_4)_2$ + 6.25 mM LiCl

to 1, the system has a more capacitive character. The *b*-value analysis was performed using the cyclic voltammetry data (Fig. 7b) between 0.25 and −0.50 V (vs. Mg/Mg^{2+}). The *b* value of the reduction peaks is 0.9 which indicates that the capacity of the magnesium-lithium battery has more pseudocapacitance characteristics than the mixed controlled process. In [11], the authors state that for the TiO_2-B electrode, approximately 74% of the total capacitance is pseudocapacitance at a scan rate of 2 mV s^{-1}. It should be noted that in many studies [10, 12, 45], it was concluded that electrodes based on titanium oxide exhibit a mixed character with a predominance of pseudocapacitive components. In addition, when using TiO_2-B in lithium-ion batteries, this material showed a large percentage of capacity from pseudocapacity. The authors of [11] assumed that the pseudocapacitive nature of the TiO_2-B electrode in mixed batteries can be explained by the large contribution of Li ions.

The charge–discharge measurements have been investigated in following cell TiO_2||0.05 M $Mg(ClO_4)_2$ + 0.009 M LiCl/AN||Mg (Fig. 8) to determine the specific capacity of TiO_2 in the Mg^{2+}/Li^+ mixed electrolyte.

Figure 8a shows the charge–discharge curves of the MLIB cell at a current density of 35 mA g^{-1}. TiO_2 exhibits a large capacity of approximately 380 mAh g^{-1}. However, after the first charging, the specific capacity of the discharge process decreased dramatically to 50 mAh g^{-1}. This capacity fading may be related to the formation of a solid electrolyte interphase (SEI) film and some side reactions [10].

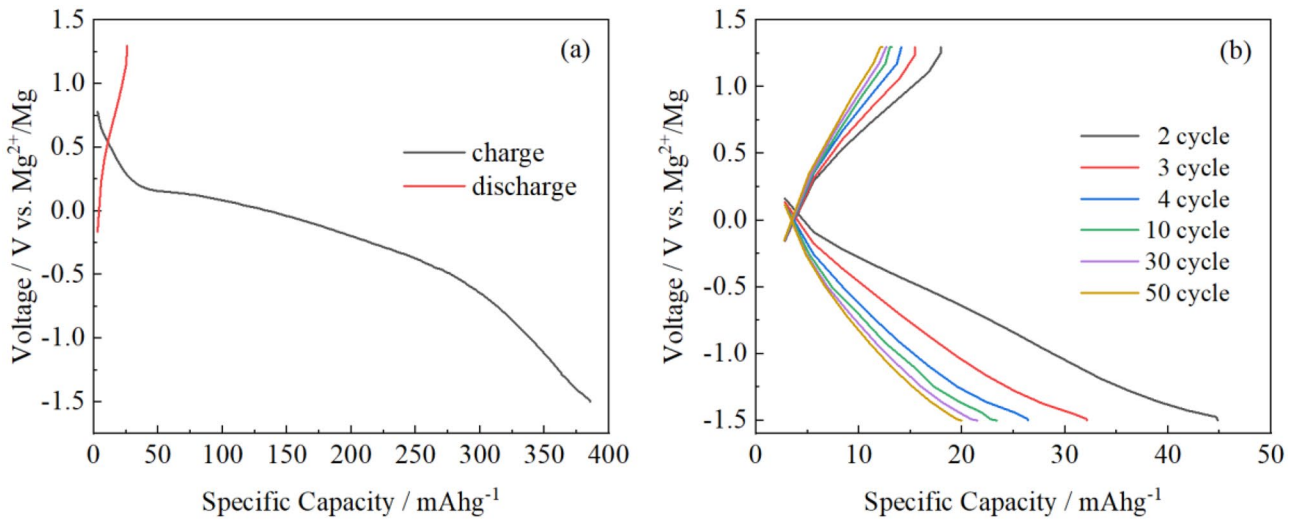


Fig. 8 Charge–discharge profiles of the TiO_2 in MLIB mixed electrolyte cells in first (**a**) and subsequent cycles (**b**)

Wang and Jin determined experimentally and by DFT calculations that the oxygen vacancies (OVs) can enhance the electrical conductivity and increase the number of active sites for Mg^{2+} storage [33]. The presence of OVs in B-TiO_2 can significantly improve the electrochemical performance of rechargeable Mg batteries. In addition, the cyclic voltammograms presented in [33], as in our work, do not have pronounced anodic and cathodic peaks, which indicates slow kinetics of the electrochemical reactions. However, the mechanism and kinetics of intercalation and deintercalation of magnesium into titanium oxide have not been sufficiently studied. In our case, the mechanism of magnesium intercalation and deintercalation is complicated by the presence of Li^+ ions.

To explain the slight increase in capacity after the introduction of LiCl into the electrolyte (Table 1), we consider the mechanism proposed in [10]. According to the charge–discharge curve shown in Fig. 8a, there are significant differences in the charge and discharge capacities, which can be explained by the saturation of TiO_2 with lithium. That is, during the first cycle, charge transfer mainly occurred owing to the discharge of lithium with the further formation of Li_2TiO_3. It is also clear from Fig. 8b that in further cycling (cycles 2–4), the drop in capacity is not very noticeable, and the process of insertion of magnesium into the electrode material can be explained by the following [10]:

$$10Li_2TiO_3 + 4Mg^{2+} + 8e^- = Mg_4LiTi_5O_{12} + Li_7Ti_5O_{12} + 6Li_2O$$

This transformation from the Li_2TiO_3 phase to an irreversible product Li_2O may be one of the reasons for the irreversible capacity during discharge [10]. After the fourth cycle, TiO_2 presents a charging capacity of 26 and 15 mAh g^{-1} in discharge.

Moreover, work [10] provides data on the decrease in capacity after the first cycling from 146.6 to 81.2 mAh g^{-1} (as in our case). However, after the 11th cycle, the capacity was restored to 112.2 mAh g^{-1}, which is explained by the activation process of the electrode material as follows:

$$Mg_4LiTi_5O_{12} \rightleftarrows Mg_{2.5}LiTi_5O_{12} + 1.5Mg^{2+} + 3e^-$$

To verify this assumption, we obtained charge and discharge curves for up to 50 cycles (Fig. 8b). Unfortunately, in our case, we did not observe a noticeable increase in capacity when cycling for 10 or more cycles, and after 50 cycles, it remained approximately the same, which was approximately 21 mAh g^{-1} when charged and 13 mAh g^{-1} when discharged. This can be explained by the difference in the nature of the SEI associated with the composition of the electrolyte. It is assumed that after activation, a new spinel magnesium titanate (Mg_4Li and $Mg_{2.5}Li$) is formed in the electrodes, and an electrochemical reaction occurs with the already formed Mg_4Li and $Mg_{2.5}Li$ phases, which further serve as active materials:

$$Mg_{2.5}Li + 1.5Mg^{2+} + 3e \overset{intercalation/deintercalation}{\Longleftrightarrow} Mg_4Li$$

In conclusion, it can be noted that the specific capacity of the material is much higher than that of TiO_2 nanotubes [31] but is still lower than that reported in other studies [10–12, 45].

Conclusion

Self-prepared TiO_2 using a solid-state chemical reaction showed a high capacity of approximately 380 mAh g^{-1} for the first cycle. The addition of Cl^- anions decreases the charge-transfer resistance, thereby facilitating the diffusion of magnesium ions into TiO_2. The optimal concentration of the Cl^- anion (in this work, the Cl^- anion was added in the form of LiCl) was determined to be 9 mM. At this concentration, Mg ions demonstrate high diffusivity ($2.90 \times 10^{-10} cm^2 s^{-1}$). A further increase in the LiCl concentration to 25 mM decreased the diffusion coefficient ($6.05 \times 10^{-11} cm^2 s^{-1}$). From the EIS data, the charge-transfer rate constant was calculated ($k_s^{exp} = 1.05 \times 10^{-8}$ cm s^{-1}), which was lower than that of the TiO_2 electrode prepared by the hydrothermal method. It may seem that the TiO_2 obtained by solid-state chemical reaction has sluggish kinetics. However, it is faster than that for TiO_2 nanotubes, which have a rate constant in the range of 1.55×10^{-10} cm s^{-1}. To determine the contribution of capacitance to the total current, an analysis of the dependence of log(*j*)–log(*v*) was performed. From the slope–*b* of the linear dependence, it was found that the capacity of the magnesium-lithium battery had a more pseudocapacitance character than the mixed control (both charge-discharge of the double layer and diffusion of Mg ions). In conclusion, TiO_2 synthesized via a solid-state chemical reaction is useful as an anode for rechargeable batteries in a perchlorate/chloride mixed electrolyte in acetonitrile. Pure perchlorate electrolytes in acetonitrile clearly demonstrate a non-Faradaic nature.

Acknowledgements The authors thank Ms. Magrife Manarbek from Satbayev University for her language corrections during the preparation of the manuscript.

Funding The work was funded by the Ministry of Science and Higher Education of the Republic of Kazakhstan—AP09260383.

References

1. Arthur TS, Singh N, Matsui M (2012) Electrodeposited Bi, Sb and Bi1-xSbx alloys as anodes for Mg-ion batteries. Electrochem Commun 16:103–106. https://doi.org/10.1016/j.elecom.2011.12.010
2. Koketsu T, Ma J, Morgan BJ et al (2017) Reversible magnesium and aluminium ions insertion in cation-deficient anatase TiO_2. Nat Mater 16:1142–1148. https://doi.org/10.1038/nmat4976
3. Rajput NN, Qu X, Sa N et al (2015) The coupling between stability and ion pair formation in magnesium electrolytes from first-principles quantum mechanics and classical molecular dynamics. J Am Chem Soc 137:3411–3420. https://doi.org/10.1021/jacs.5b01004
4. Yang J, Li J, Gong W, Geng F (2021) Genuine divalent magnesium-ion storage and fast diffusion kinetics in metal oxides at room temperature. Proc Natl Acad Sci 118(38):e2111549118. https://doi.org/10.1073/pnas.2111549118
5. Yang R, Zhang F, Lei X et al (2020) Pseudocapacitive Ti-doped niobium pentoxide nanoflake structure design for a fast kinetics anode toward a high-performance Mg-ion-based dual-ion battery. ACS Appl Mater Interfaces 12:47539–47547. https://doi.org/10.1021/acsami.0c13045
6. Meng Y, Wang D, Zhao Y et al (2017) Ultrathin TiO_2-B nanowires as an anode material for Mg-ion batteries based on a surface Mg storage mechanism. Nanoscale 9:12934–12940. https://doi.org/10.1039/C7NR03493H
7. Shterenberg I, Salama M, Yoo HD et al (2015) Evaluation of $(CF_3SO_2)_2N^-$ (TFSI) based electrolyte solutions for Mg batteries. J Electrochem Soc 162:A7118–A7128. https://doi.org/10.1149/2.0161513jes
8. Huie MM, Bock DC, Takeuchi ES et al (2015) Cathode materials for magnesium and magnesium-ion based batteries. Coord Chem Rev 287:15–27. https://doi.org/10.1016/j.ccr.2014.11.005
9. Murgia F, Weldekidan ET, Stievano L et al (2015) First investigation of indium-based electrode in Mg battery. Electrochem Commun 60:56–59. https://doi.org/10.1016/j.elecom.2015.08.007
10. Wu N, Yang YJ, Zhang QY et al (2020) A layered titanium-based transition metal oxide as stable anode material for magnesium-ion batteries. J Mater Sci 55:16674–16682. https://doi.org/10.1007/s10853-020-05195-0
11. Meng Y, Wang D, Wei Y et al (2017) Competition between insertion of Li^+ and Mg^{2+}: an example of TiO_2-B nanowires for Mg rechargeable batteries and Li^+/Mg^{2+} hybrid-ion batteries. J Power Sources 346:134–142. https://doi.org/10.1016/j.jpowsour.2017.02.033
12. Fu Q, Azmi R, Sarapulova A et al (2018) Electrochemical and structural investigations of different polymorphs of TiO_2 in magnesium and hybrid lithium/magnesium batteries. Electrochim Acta 277:20–29. https://doi.org/10.1016/j.electacta.2018.04.200
13. Su S, NuLi Y, Huang Z et al (2016) A high-performance rechargeable Mg^{2+}/Li^+ hybrid battery using one-dimensional mesoporous TiO_2(B) nanoflakes as the cathode. ACS Appl Mater Interfaces 8:7111–7117. https://doi.org/10.1021/acsami.6b00106
14. Gao T, Han F, Zhu Y et al (2015) Hybrid Mg^{2+}/Li^+ battery with long cycle life and high rate capability. Adv Energy Mater 5:1401507. https://doi.org/10.1002/aenm.201401507
15. Cheng Y, Shao Y, Zhang J-G et al (2014) High performance batteries based on hybrid magnesium and lithium chemistry. Chem Commun 50:9644–9646. https://doi.org/10.1039/C4CC03620D
16. Xue X, Song X, Yan W et al (2022) Cooperative cationic and anionic redox reactions in ultrathin polyvalent metal selenide nanoribbons for high-performance electrochemical magnesium-ion storage. ACS Appl Mater Interfaces 14:48734–48742. https://doi.org/10.1021/acsami.2c14237
17. Xue X, Song X, Tao A et al (2023) Boosting the cycling stability of rechargeable magnesium batteries by regulating the compatibility between nanostructural metal sulfide cathodes and non-nucleophilic electrolytes. Nano Res 16:2399–2408. https://doi.org/10.1007/s12274-022-4932-z
18. Xue X, Chen R, Song X et al (2021) Electrochemical Mg^{2+} displacement driven reversible copper extrusion/intrusion reactions for high-rate rechargeable magnesium batteries. Adv Funct Mater 31(10):2009394. https://doi.org/10.1002/adfm.202009394
19. Wang Y, Wang C, Yi X et al (2019) Hybrid Mg/Li-ion batteries enabled by Mg^{2+}/Li^+ co-intercalation in VS_4 nanodendrites. Energy Stor Mater 23:741–748. https://doi.org/10.1016/j.ensm.2019.06.001
20. Attias R, Chae MS, Dlugatch B et al (2020) The role of surface adsorbed Cl^- complexes in rechargeable magnesium batteries. ACS Catal 10:7773–7784. https://doi.org/10.1021/acscatal.0c01956
21. Shao Y, Gu M, Li X et al (2014) Highly reversible Mg insertion in nanostructured Bi for Mg ion batteries. Nano Lett 14:255–260. https://doi.org/10.1021/nl403874y
22. DiLeo RA, Zhang Q, Marschilok AC et al (2014) Composite anodes for secondary magnesium ion batteries prepared via electrodeposition of nanostructured bismuth on carbon nanotube substrates. ECS Electrochem Lett 4:A10–A14. https://doi.org/10.1149/2.0081501eel
23. Singh N, Arthur TS, Ling C et al (2013) A high energy-density tin anode for rechargeable magnesium-ion batteries. Chem Commun 49:149–151. https://doi.org/10.1039/C2CC34673G
24. Periyapperuma K, Tran TT, Purcell MI, Obrovac MN (2015) The reversible magnesiation of Pb. Electrochim Acta 165:162–165. https://doi.org/10.1016/j.electacta.2015.03.006
25. Hua X, Liu Z, Bruce PG, Grey CP (2015) The morphology of TiO_2 (B) nanoparticles. J Am Chem Soc 137:13612–13623. https://doi.org/10.1021/jacs.5b08434
26. Kubiak P, Pfanzelt M, Geserick J et al (2009) Electrochemical evaluation of rutile TiO_2 nanoparticles as negative electrode for Li-ion batteries. J Power Sources 194:1099–1104. https://doi.org/10.1016/j.jpowsour.2009.06.021
27. Akolkar R (2014) Modeling dendrite growth during lithium electrodeposition at sub-ambient temperature. J Power Sources 246:84–89. https://doi.org/10.1016/j.jpowsour.2013.07.056
28. Giannuzzi R, Manca M, De Marco L et al (2014) Ultrathin TiO_2(B) nanorods with superior lithium-ion storage performance. ACS Appl Mater Interfaces 6:1933–1943. https://doi.org/10.1021/am4049833
29. Wu N, Lyu YC, Xiao RJ et al (2014) A highly reversible, low-strain Mg-ion insertion anode material for rechargeable Mg-ion batteries. NPG Asia Mater 6:e120–e120. https://doi.org/10.1038/am.2014.61
30. Luo L, Zhen Y, Lu Y et al (2020) Structural evolution from layered $Na_2Ti_3O_7$ to $Na_2Ti_6O_{13}$ nanowires enabling a highly reversible anode for Mg-ion batteries. Nanoscale 12:230–238. https://doi.org/10.1039/C9NR08003A
31. Jumanova R, Rakhymbay G, Abildina A et al (2023) Nanostructured TiO_2 as anode material for magnesium-ion batteries. J Solid State Electrochem 27:223–233. https://doi.org/10.1007/s10008-022-05307-7
32. Abildina AK, Avchukir K, Dzhumanova RZ et al (2021) Preparation and electrochemical characterization of TiO_2 as an anode material for magnesium-ion batteries. Bull Karaganda Univ Chemistry Ser 104:104–116. https://doi.org/10.31489/2021Ch4/104-116
33. Liu F, Cao G, Ban J et al (2022) Recent advances based on Mg anodes and their interfacial modulation in Mg batteries. J Magnes Alloy 10:2699–2716. https://doi.org/10.1016/j.jma.2022.09.004
34. Li Y, Cao Y, Jia D (2014) A general strategy for synthesis of metal nanoparticles by a solid-state redox route under ambient conditions. J Mater Chem A 2:3761. https://doi.org/10.1039/c3ta14427e

35. Wang Y, Tang X, Cao S et al (2019) A novel method to synthesis titanium dioxide(B)/anatase composite oxides by solid-state chemical reaction routes for promoting Li^+ insertion. Results Phys 14:102451. https://doi.org/10.1016/j.rinp.2019.102451
36. Wang Y, Cao Y, Li Y et al (2014) Directed synthesis of TiO_2 nanorods and their photocatalytic activity. Ceram Int 40:11735–11742. https://doi.org/10.1016/j.ceramint.2014.03.187
37. Wang JF, Zhang JJ, He DN (2018) Flower-like TiO_2-B particles wrapped by graphene with different contents as an anode material for lithium-ion batteries. Nano Struct Nano Objects 15:216–223. https://doi.org/10.1016/j.nanoso.2018.03.008
38. Lee SH, DiLeo RA, Marschilok AC et al (2014) Sol gel based synthesis and electrochemistry of magnesium vanadium oxide: a promising cathode material for secondary magnesium ion batteries. ECS Electrochem Lett 3:A87–A90. https://doi.org/10.1149/2.0021408eel
39. Imamura D, Miyayama M, Hibino M, Kudo T (2003) Mg intercalation properties into V_2O_5 gel/carbon composites under high-rate condition. J Electrochem Soc 150:A753. https://doi.org/10.1149/1.1571531
40. Avchukir K, Burkitbayeva BD, Argimbayeva AM et al (2018) The kinetics of indium electroreduction from chloride solutions. Russ J Electrochem 54:1096–1103. https://doi.org/10.1134/S1023193518120042
41. Avchukir K, Burkitbayeva BD, Vacandio F et al (2019) Influence of tetrabutylammonium chloride on the electrodeposition of indium from chloride solution on a glassy carbon electrode. J Electroanal Chem 842:176–183. https://doi.org/10.1016/j.jelechem.2019.04.078
42. Supiyeva Z, Avchukir K, Pavlenko V et al (2020) The investigation of electroreduction of AuCl-4 in the case of gold electrosorption using activated carbon. Mater Today Proc 25:33–38. https://doi.org/10.1016/j.matpr.2019.11.013
43. Mansurov Z, Supiyeva Z, Avchukir K et al (2019) Investigation of gold electrosorption onto gold and carbon electrodes using an electrochemical quartz crystal microbalance. Eurasian Chem J 21:283. https://doi.org/10.18321/ectj885
44. Muller GA, Cook JB, Kim HS et al (2015) High performance pseudocapacitor based on 2D layered metal chalcogenide nanocrystals. Nano Lett 15:1911–1917. https://doi.org/10.1021/nl504764m
45. Le TS, Hoa TH, Truong DQ (2019) Shape-controlled F-doped TiO_2 nanocrystals for Mg-ion batteries. J Electroanal Chem 848:113293. https://doi.org/10.1016/j.jelechem.2019.113293

Publisher's Note Springer Nature remains neutral with regard to jurisdictional claims in published maps and institutional affiliations.

Springer Nature or its licensor (e.g. a society or other partner) holds exclusive rights to this article under a publishing agreement with the author(s) or other rightsholder(s); author self-archiving of the accepted manuscript version of this article is solely governed by the terms of such publishing agreement and applicable law.